OPEN ACCESS
JOURNAL OF ADVANCED DIELECTRICS
Vol. 13, No. 2 (2023) 2250022 (7 pages)

DOI: 10.1142/S2010135X22500229

Fabrication plate-like $BaBi_4Ti_4O_{15}$ single-crystalline particles by the molten salt synthesis method

Xiaoying Feng*, Bei Xu*,§, Xiaoyu Xu*, Penghui Chen*, Zhuozhao Wu†, Duo Teng‡,¶,**, Jie Xu* and Feng Gao*,‖,**

*State Key Laboratory of Solidification Processing, MIIT Key Laboratory of Radiation Detection Materials and Devices, USI Institute of Intelligence Materials and Structure NPU-QMUL Joint Research Institute of Advanced Materials and Structure School of Materials Science and Engineering, Northwestern Polytechnical University Xi'an 710072, P. R. China

†Queen Mary University of London Engineering School, Northwestern Polytechnical University Xi' an 710072, P. R. China

‡School of Marine Science and Technology, Northwestern Polytechnical University Xi' an 710072, P. R. China

§Guangzhou Newlife New Material Co., Ltd, Guangzhou 511356, P. R. China

¶tengduo@nwpu.edu.cn

‖gaofeng@nwpu.edu.cn

Received 6 August 2022; Revised 14 September 2022; Accepted 29 October 2022; Published 7 December 2022

Plate-like single-crystalline $BaBi_4Ti_4O_{15}$ particles were synthesized by the molten salt synthesis (MSS) method. The effects of sintering temperature, holding time, and NaCl–KCl molten salt content on the phase structure and morphology of plate-like $BaBi_4Ti_4O_{15}$ particles were investigated. The results show that plate-like $BaBi_4Ti_4O_{15}$ particles can be synthesized when the sintering temperature is above 800°C. The size of particles increases with increasing sintering temperature and molten salt content. Largely anisotropic plate-like $BaBi_4Ti_4O_{15}$ particles with diameter ≥10 μm and thickness of ~0.3 μm can be obtained under the optimum process parameters. The crystal structure of $BaBi_4Ti_4O_{15}$ was determined as $A2_1am$ by TEM, which should be attributed to the Bi^{3+} and Ba^{2+} diffusing into $[TiO_6]$ octahedrons.

Keywords: Molten salt synthesis method; calcining condition; salts content; microplatelets; anisotropy.

1. Introduction

Bismuth layer-structured ferroelectrics (BLSF) formulated as Aurivillius compounds $(Bi_2O_2)^{2+}(A_{m-1}B_mO_{3m+1})^{2-}$ (Refs. 1–3) are promising candidates in high-temperature piezoelectric applications because of high Curie temperature and mechanical quality factor, low dielectric constant and coupling coefficient.[4,5] The Aurivillius $BaBi_4Ti_4O_{15}$ (BBT) particles with *m* equal to 4 formed by alternately stacked $[Bi_2O_2]^{2+}$ monolayers and pseudo-perovskite $[BaBi_2Ti_4O_{13}]^{2-}$ quadruple sheets in the c direction, and its Curie temperature is 417°C. However, the low piezoelectric constant (12 pC/N) restricted the applications of the material.[6,7]

It is reported that the method of controlling microstructure with grain orientation makes it possible to obtain textured ceramics with the desired properties. As an alternative to hot pressing and hot forging techniques, reactive-templated grain growth (RTGG) offers the possibility of fabricating textured ceramics.[8] To prepare the textured ceramics, a small portion of anisotropic templates needs to be aligned in green bodies. The morphology and crystal symmetry of the template particles determine the texture orientation. Therefore, synthesizing anisotropic templates with a proper scale is a key procedure in preparing textured ceramics.

Molten salt synthesis (MSS) method has been widely applied in the recent years to prepare particles with specific morphology.[9,10] This method has advantages of simplicity in the process equipment, versatility and large-scale synthesis, and friendly environment, which provides an excellent approach to synthesizing high pure oxide powders with controllable compositions and morphologies. In this approach, inorganic molten salt is served as the reaction medium to enhance the reaction rate and reduce the reaction temperature of the reactant oxides. Adopting this method, anisotropic particles of $Sr_3Ti_2O_7$,[11] $SrTiO_3$,[12] $BaTiO_3$,[13] $Bi_4Ti_3O_{12}$,[14] $KSr_2Nb_5O_{15}$,[15] etc., have been produced successfully. However, the $BaBi_4Ti_4O_{15}$ particles with anisotropic

**Corresponding authors.

morphology, especially about the detailed description of the process parameters of MSS, have not been systematically investigated and understood. In this work, MSS of plate-like $BaBi_4Ti_4O_{15}$ particles will be described. The effects of sintering temperature, holding time, and molten salt content on the phase structure and morphology of plate-like $BaBi_4Ti_4O_{15}$ particles will be reported.

2. Experimental Procedure

The Aurivillius BBT particles were synthesized using the MSS method, according to Eq. (1). The high-purity $BaCO_3$ (99%), Bi_2O_3 (99%), TiO_2 (99%), NaCl (99%), and KCl (99%) powders (Sinopharm Chemical Reagent Co., Ltd) were used as raw materials. Stoichiometric amounts of $BaCO_3$, Bi_2O_3 and TiO_2 were mixed with NaCl and KCl molten salts via planetary ball milling for 12 h in alcohol. The NaCl and KCl were weighed at a molar ratio of 1:1, and to raw materials ($R_{S\text{-}R}$) of 1:1. After drying, the mixtures were heated at 800°C, 900°C, 950°C, 1000°C and 1050°C for 4 h. Then, the obtained substances were washed to remove salts several times using hot deionized water. To investigate the influence of holding time and the molten salt content, the reactants with $R_{S\text{-}R}$ of 1:1 were sintered for 2 h, 4 h, 6 h, and 8 h, and then the $R_{S\text{-}R}$ was chosen as 0.2:1, 0.5:1, 1:1, 1.2:1, 1.5:1 and 1.8:1, respectively.

$$BaCO_3 + 2Bi_2O_3 + 4TiO_2 \rightarrow BaBi_4Ti_4O_{15} + CO_2\uparrow. \quad (1)$$

The differential scanning calorimetry measurements (DSC204HP) of particles were performed in air at a heating rate of 10°C/min from 100°C to 1200°C. The phase structure was determined by X-ray diffraction (XRD) (X'pert PRO, Holand) using Cu Ka radiation. The morphology of particles was observed by scanning electron microscopy (SEM) (Quanta 600 FEG, FEI, America). The lattice structure of the plate-like particles was confirmed by micro-electron-beam diffraction linked to transmission electron microscopy (TEM) (JEM-200CX, JEOL, Japan).

3. Results and Discussion

Figure 1 shows the DSC analysis of reactants preparing $BaBi_4Ti_4O_{15}$ particles by MSS. It can be seen that there are obvious endothermic peaks at about 550°C, 650°C, and 950°C. It is known that the raw TiO_2 powders are anatase structures, which would transform into rutile structures at about 550°C. The endothermic peak near 650°C corresponds to the eutectic point of NaCl–KCl salt. The endothermic peak near 950°C starts at 800°C and ends at 1000°C, which means that the $BaBi_4Ti_4O_{15}$ compound nucleates and grows.

Figure 2 shows XRD pattern of $BaBi_4Ti_4O_{15}$ particles sintered at different temperatures. It can be found that from 800°C to 1050°C, the main peaks are corresponding to $BaBi_4Ti_4O_{15}$, and a few peaks of $Ba_2Bi_4Ti_5O_{18}$ and $Bi_4Ti_3O_{12}$

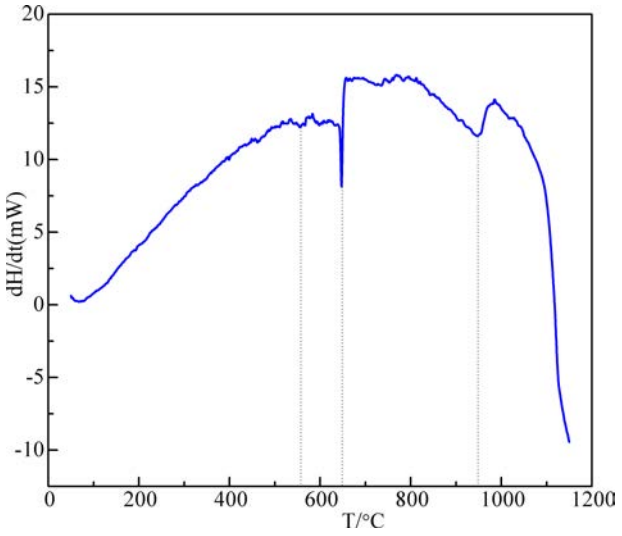

Fig. 1. The DSC analysis of the reactants of $BaBi_4Ti_4O_{15}$ particles.

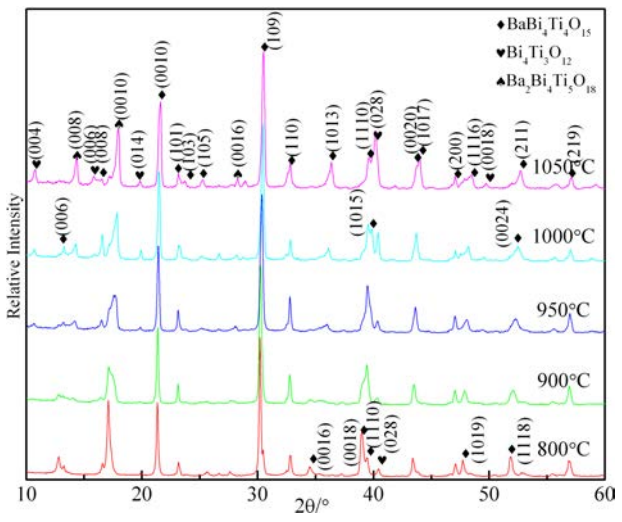

Fig. 2. XRD patterns of $BaBi_4Ti_4O_{15}$ particles prepared at different sintering temperatures.

phases can be found. It suggests that due to the similar crystal structure of these compounds, $Bi_4Ti_3O_{12}$ and $Ba_2Bi_4Ti_5O_{18}$ were synthesized simultaneously as shown in Eqs. (2) and (3).

$$2Bi_2O_3 + 3TiO_2 \rightarrow Bi_4Ti_3O_{12}, \quad (2)$$

$$2BaCO_3 + 2Bi_2O_3 + 5TiO_2 \rightarrow Ba_2Bi_4Ti_5O_{18} + 2CO_2\uparrow. \quad (3)$$

The XRD pattern shows that the diffraction peak intensities of the [00l] crystal planes were enhanced with the temperature increase, which indicated that the single-crystalline $BaBi_4Ti_4O_{15}$ microplatelets are preferentially oriented [001].

The SEM images of the samples are shown in Fig. 3. As the sintering temperature increases, the size of microplatelets has a tendency of increasing. When the sintering temperature is 800°C, the microplatelets have diameters of ~ 5 μm

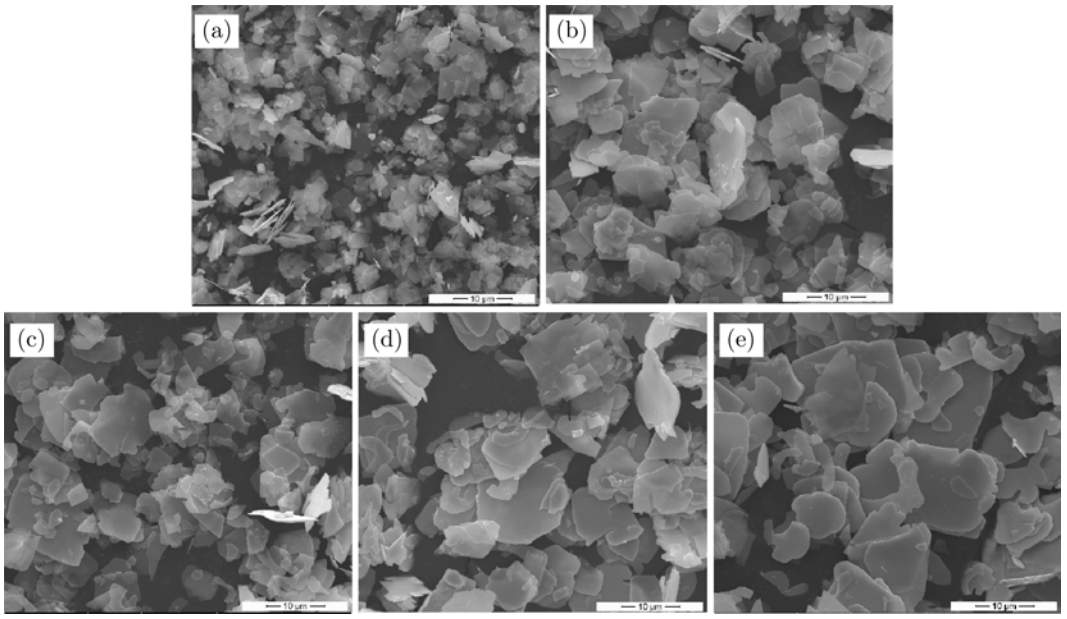

Fig. 3. SEM images of $BaBi_4Ti_4O_{15}$ microplatelets sintered at different temperatures: (a) 850°C, (b) 900°C, (c) 950°C, (d) 1000°C and (e) 1050°C.

and thicknesses of ~ 0.1 μm. When the sintering temperature arrives at 900–950°C, the diameter increases to ~ 10 μm, obviously. At 1000°C, the microplatelets' size is more homogeneous, the diameter is larger than 10 μm and the thickness is ~0.3 μm. Above 1000°C, the diameter and thickness are a litter larger than that of 1000°C. Taking into consideration the phase structure and the particle size of the microplatelets, 1000°C is chosen as the best sintering temperature.

Figure 4 shows XRD pattern of $BaBi_4Ti_4O_{15}$ particles prepared at 1000°C for different holding times. The particles consisted of the main phase $BaBi_4Ti_4O_{15}$ and some other impurities. When the holding time is 2 h, the relative intensity of (0010) and (0020) peaks is low. When the holding time reaches 4 h, the relative intensity of (00*l*) peaks increases rapidly and continues to increase the holding time, and the (00*l*) peaks do not have obvious change.

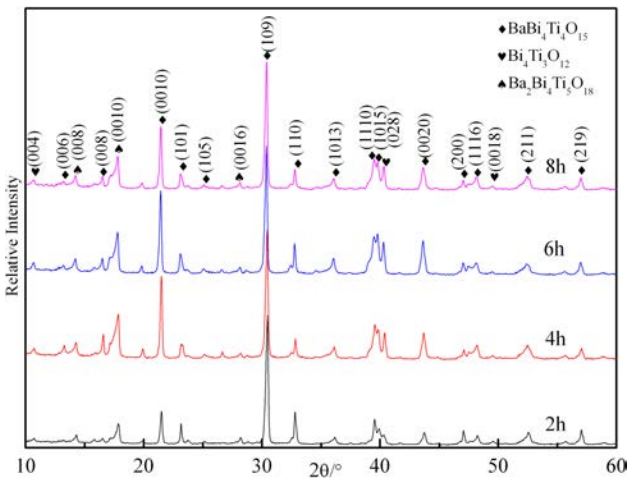

Fig. 4. XRD patterns of $BaBi_4Ti_4O_{15}$ particles prepared at 1000°C for different holding times.

From the SEM images in Fig. 5, it is observed that the size of $BaBi_4Ti_4O_{15}$ particles increases when the holding time increases to 4 h and then increases a little as the holding time continues to increase. The magnified SEM images show that the thickness of particles with a holding time of 2 h is ~0.15 μm and that with a holding time of 4 h is ~0.3 μm. When the holding time increases to 4 h, 6 h or 8 h, the thicknesses do not change.

Mohammad E. Ebrahimi *et al*. pointed out that the MSS method can be viewed as four sequential processes: Reactant dissolution, reactant transport through the melt, nucleation of the product and growth of the product onto existing nuclei.[16] In the process of the system from room temperature to 1000°C, the samples have nucleated, and then the crystal particles grow in the direction of diameter and thickness on the nuclei. Owing to the larger energy barrier along *c*-axis than *a*- and *b*-axes, the growth rate is lower in the thickness direction.[17] As the microcrystal grows, the ion concentration in the molten salt decreases, leading that potential energies cannot be provided sufficiently, blocking that $BaBi_4Ti_4O_{15}$ crystals grow along the thickness direction, thus the thickness with a holding time of 4 h has saturated. And then, the diffusion and rearrangement of the ions in the diameter direction also saturate, which can explain that the relative intensity of (00*l*) and the particle size do not change too much. According to the phenomenon, it is thought that 4 h is the optimal holding time.

Figure 6 shows the XRD pattern of $BaBi_4Ti_4O_{15}$ particles prepared with different ratios of NaCl–KCl to raw

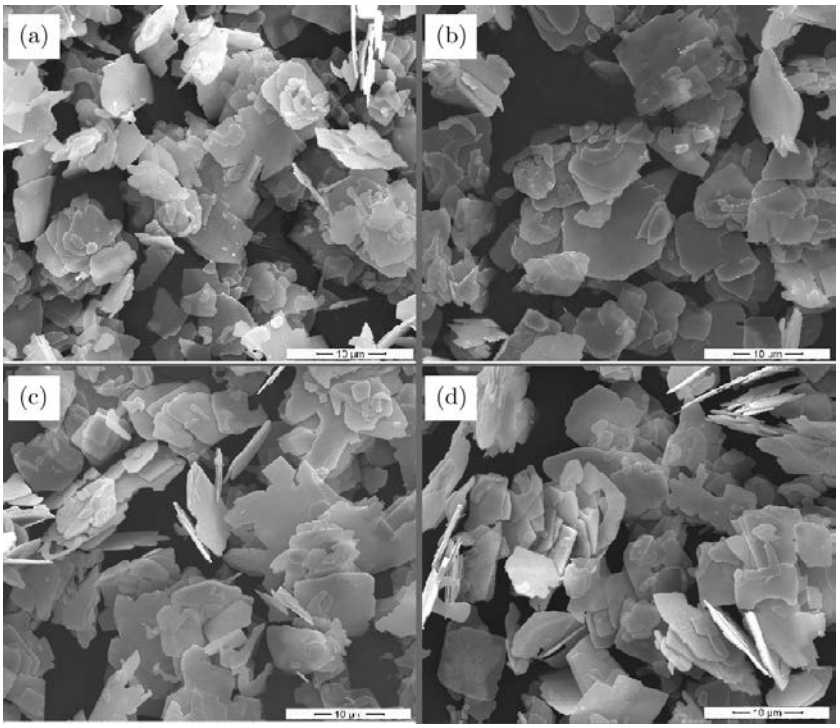

Fig. 5. SEM images of $BaBi_4Ti_4O_{15}$ particles prepared at 1000°C for different holding time: (a) 2 h (b) 4 h (c) 6 h and (d) 8 h.

materials ($R_{S\text{-}R}$) at 1000°C. It is found that there are also some $Ba_2Bi_4Ti_5O_{18}$ and $Bi_4Ti_3O_{12}$ phases, which indicate that changing the $R_{S\text{-}R}$ does not affect phase composition. When the $R_{S\text{-}R}$ increases, the relative intensity of (0010) and (0020) peaks changes a lot. Lotgering proposed the orientation degree (f) to estimate the degree of anisotropy for ceramics.[18] The relative intensities of (00l) peaks can reflect the <00l> orientation degree qualitatively. In order to express the orientation degree, the intensive ratio of (0010)–(109) and (0020)–(109) is calculated as in Fig. 7. As the $R_{S\text{-}R}$ increases, the orientation degree of particles with $R_{S\text{-}R}$ equal to 0.5:1 is a little higher and that of 1:1 increases rapidly. When $R_{S\text{-}R}$ reaches 1.2:1, the orientation degree has the highest value. However, when the $R_{S\text{-}R}$ continues to increase, the orientation degree decreases, indicating that the $R_{S\text{-}R}$ of 1.2:1 leads to the highest (00l) orientation degree.

Figure 8 shows SEM images of $BaBi_4Ti_4O_{15}$ particles prepared with different $R_{S\text{-}R}$ values. All the microplatelets appear plate-like, proving the anisotropic growth. It is also found that the diameter changes a lot as the content ratio of salt increases. When the $R_{S\text{-}R}$ is 0.2:1, the diameter of

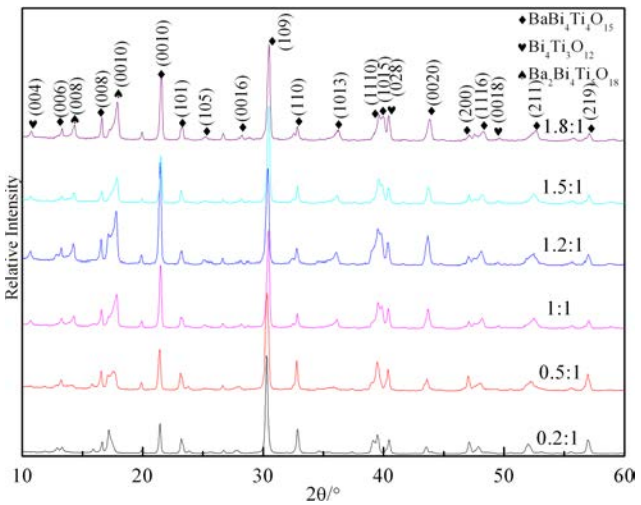

Fig. 6. XRD patterns of $BaBi_4Ti_4O_{15}$ prepared with different ratios of NaCl–KCl to raw materials ($R_{S\text{-}R}$).

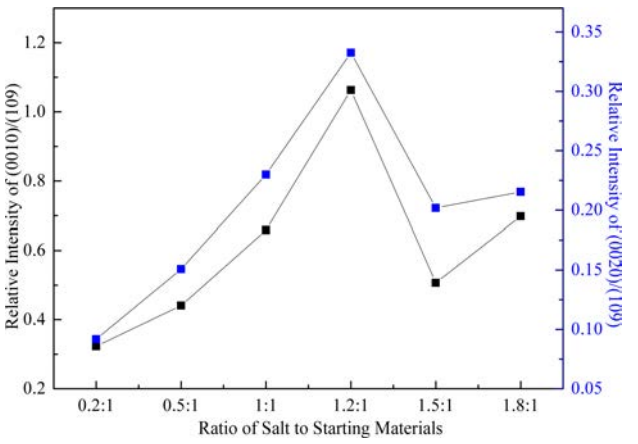

Fig. 7. The relative intensity ratio of (0010) to (109) and (0020) to (109) of $BaBi_4Ti_4O_{15}$ prepared with different ratios of NaCl–KCl to raw materials ($R_{S\text{-}R}$).

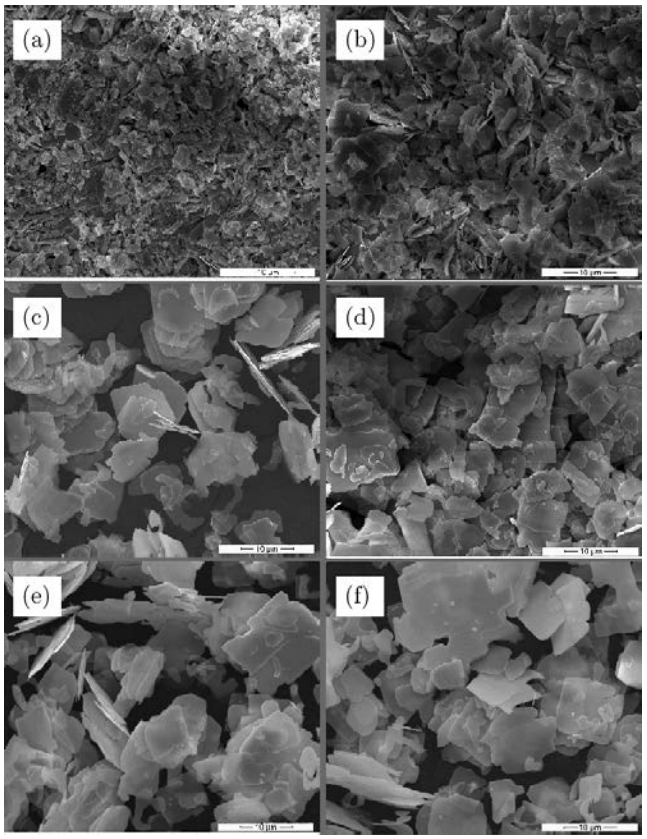

Fig. 8. SEM images of $BaBi_4Ti_4O_{15}$ particles prepared with different $R_{S\text{-}R}$ values: (a) 0.2:1, (b) 0.5:1, (c) 1:1, (d) 1.2:1, (e) 1.5:1 and (f) 1.8:1.

microplatelets is ~2 μm and the thickness of that is 0.1–0.2 μm. When the $R_{S\text{-}R}$ reaches 0.5:1, the diameter of microplatelets is ~5 μm and the thickness of that is 0.2–0.3 μm. The size of the particles will reach larger than 10 μm as the $R_{S\text{-}R}$ increases to larger than 1:1. And then, as the $R_{S\text{-}R}$ increases, the size increases slightly. However, the thickness of plates almost remains 0.2–0.3 μm.

Actually, the eutectic mixtures of NaCl–KCl are totally molten when the temperature is higher than 670°C.[19] And, the molten salt plays a role as an intermedium to promote diffusion of ions, lower the energy barrier and accelerate grain growth.[20] It has been investigated that the mobility of mass in the flux is from 1×10^{-5} to 1×10^{-8} cm^2/s and that the mobility in a solid state is just 1×10^{-18} cm^2/s. Also, the unstrained growing environment benefits the shape formation of crystals according to the crystal structure.[21] If the salt content is low, the fluid will be deficient to provide enough space for ions to diffuse, with more resistance of diffusion, which blocks the growth of the nucleus, so the size will be restricted to a small value. On the contrary, good fluidity of the molten salt will expedite diffusing velocity, making a larger quantity of the raw materials dissolved into the molten salt react completely in a shorter time. It had been reported that the optimum flux/oxides weight fraction (F) was within a certain range. Whereas, continuing to increase the salt content would debase the concentration of ions of starting materials and result in too long a distance among reactants, reducing reaction speed and growth rate to a certain degree. In this system, although the sample with $R_{S\text{-}R}$ of 1.2:1 has the highest (00*l*) peaks, the size of all the samples of which $R_{S\text{-}R}$ is larger than 1.2:1 has slight changes. It is thought that $R_{S\text{-}R}$ values of 1:1 to 1.8:1 are all feasible. However, the XRD patterns and separation of the synthesized powders from salt were taken in consideration, and the salt-to-oxide weight ratio of 1.2:1 is chosen as the optimum condition.

Due to the bismuth-layer structure, including $(Bi_2O_2)^{2+}$ on the topside and bottomside and perovskite $((BaBi_2)Ti_4O_{13})^{2-}$ in the middle, the anisotropy of the structure is so severe that the growing energy barrier of c-axis would be much higher than that along the a- and b-axes. Therefore, the effect of molten salt on the growing velocity in a- and b-axes is much larger than that in the c-axis, inducing a larger change of diameter than that of thickness.

In the process of studying this system, it has been observed that there are two kinds of particles, thinner and thicker in the products. Figure 9 shows the TEM testing results of plate-like particles. It is interesting that the pattern of selective area electron diffraction (SAED) shows that the particles are single crystals. The lattice is clear and regular with some smaller points representing the existence of a superlattice due to the periodic structure. Obviously, the two kinds of particles have different diffraction spots, especially the superlattice spots. The spot indices are determined by means of measuring the distances between the bright diffraction spots and a vector composition, and then the indices of other spots are derived. The result is that the thinner particles are $BaBi_4Ti_4O_{15}$ and the thicker particles correspond to $Bi_4Ti_3O_{12}$.

From the phase diagram between Bi_2O_3, NaCl–KCl and $BaCO_3$, the eutectic point was relatively low. At the temperature of higher than 800°C, $BaCO_3$ decomposes to BaO. BaO and Bi_2O_3 system will transform to the liquid state and the concentration of Bi^{3+} and Ba^{2+} is high in the liquid. However, the eutectic point between TiO_2 and other substances in the system is very high, so TiO_2 exists as solid-state in the reacting process. In the high-temperature molten salt system, Ba^{2+} and Bi^{3+} diffuse from solution to solid TiO_2, entering into the interstices or the surface, which leads to strains of the $[TiO_6]$ structure. Owing to the instability of edge-shared structure, the $[TiO_6]$ octahedrons distort, changing the edge-shared structure to corner-shared structure.[22] Simultaneously, in order to lower the energy of the system, the $[TiO_6]$ octahedrons rotate to form local symmetric regions, on which the reactant ions in the molten salts deposit, nucleate and grow to obtain the bismuth layer structure. The sketch map of crystal structural transition is shown in Fig. 10. In the process of crystal growth, it is easy to form miscellaneous bismuth layer structures, for the deposition of ions and growth of nucleus are greatly affected by the temperature and the concentration fields.

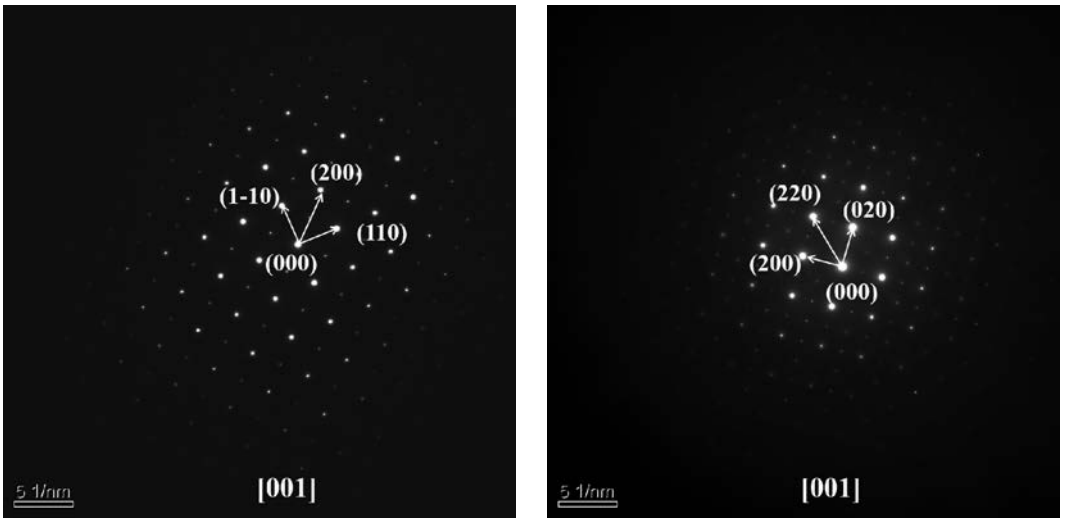

(a) (b)

Fig. 9. TEM analysis SAED of plate-like particles: (a) $BaBi_4Ti_4O_{15}$ particle and (b) $Bi_4Ti_3O_{12}$ particle.

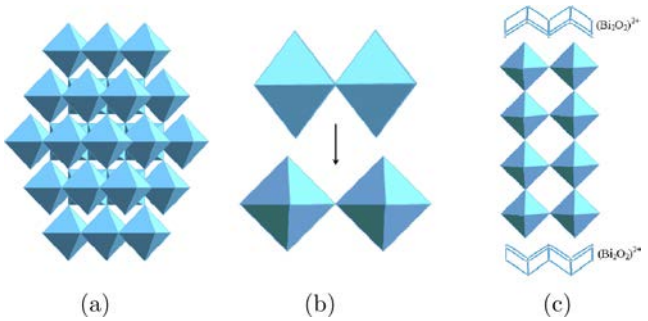

Fig. 10. Transition sketch maps of crystal structure: (a) Rutile structure seen from <111> direction; (b) common edge octahedron and corner octahedron; (c) the bismuth layer structure.

Because $Bi_4Ti_3O_{12}$ and $BaBi_4Ti_4O_{15}$ compounds are bismuth layer-structure with *m* equal to 3 and 4, respectively, the lattice constant along the c-axis of $BaBi_4Ti_4O_{15}$ is larger than that of $Bi_4Ti_3O_{12}$. Thus, it is more difficult for crystal growth of $BaBi_4Ti_4O_{15}$ along <001> direction than that of $Bi_4Ti_3O_{12}$, for the energy barrier along the *c*-axis of $BaBi_4Ti_4O_{15}$ is larger than $Bi_4Ti_3O_{12}$. Meanwhile, due to the introduction of Ba^{2+}, the mismatch between the $(Bi_2O_2)^{2+}$ layers and $[TiO_6]$ octahedrons becomes more severe.

$Bi_4Ti_3O_{12}$ and $BaBi_4Ti_4O_{15}$ are both bismuth layer structures; however, they have different diffraction spots. Thereinto, $Bi_4Ti_3O_{12}$ belongs to a tetragonal structure which is periodically arranged along <*l*00> and <*ll*0> directions, so the indices of the super lattice spots are (*l*00) and (*ll*0). However, there are only superlattice spots of (*l*00) in $BaBi_4Ti_4O_{15}$, indicating along <*ll*0>, $BaBi_4Ti_4O_{15}$ does not show periodical structure. At present, there is a debate on the structure of $BaBi_4Ti_4O_{15}$. Some considered it as a tetragonal structure (I4/mmm), while Brendan J. Kennedy *et al*. reported that $BaBi_4Ti_4O_{15}$ at room temperature was not tetragonal but the orthorhombic $A2_1am$ structure.[23,24] And, the TEM results prove that the $BaBi_4Ti_4O_{15}$ lattice structure in this work is not I4/mmm, but $A2_1am$ and $[TiO_6]$ octahedrons distort.

4. Conclusions

Plate-like $BaBi_4Ti_4O_{15}$ particles that have diameters ≥10 μm and thicknesses of 0.3 μm were prepared by one-step MSS successfully. The optimal preparing process is sintering at 1000°C for 4 h with the weight ratio of salts to raw materials equal to 1.2:1. It is observed that there are two kinds of particles; the thinner particles are $BaBi_4Ti_4O_{15}$ and the thicker particles correspond to $Bi_4Ti_3O_{12}$. The crystal structure of $BaBi_4Ti_4O_{15}$ was determined as $A2_1am$. The mechanism forming bismuth layer compound is that: (1) $[TiO_6]$ octahedrons change from edge-shared state to corner-shared structure; (2) Bi^{3+} and Ba^{2+} diffuse from the liquid into $[TiO_6]$ octahedrons to deposit; (3) corner-shared $[TiO_6]$ octahedrons rotate to form local symmetric regions; (4) the nuclei grow.

Acknowledgments

This work was financially supported by the China-Poland International Collaboration Fund of National Natural Science Foundation of China (51961135301), the National Natural Science Foundation of China (12074318 and 52072301), the International Cooperation Foundation of Shaanxi Province (2022KW-34), the Undergraduate Innovation and Entrepreneurship Training Program of Shaanxi Province (S202210699511) and the '111' Project (B20028). We would like to thank the Analytical & Testing Center of Northwestern Polytechnical University for the measurements of XRD, SEM, TEM and valuable discussion.

References

[1]F. Li, L. Jin, Z. Xu and S. Zhang, Electrostrictive effect in ferroelectrics: An alternative approach to improve piezoelectricity, *Appl. Phys. Rev*. **1**, 011103 (2014).

[2]P. K. Panda, Review: Environmental friendly lead-free piezoelectric materials, *J. Mater. Sci.* **44**, 5049 (2009).

[3]S. Zhang, F. Li, X. Jiang, J. Kim, J. Luo and X. Geng, Advantages and challenges of relaxor-$PbTiO_3$ ferroelectric crystals for electroacoustic transducers -A review, *Prog. Mater. Sci.* **68**, 1 (2015).

[4]S. K. Rout and P. K. Barhai, Anisotropic eielectric and electrical properties of hot-forged $SrBi_4Ti_4O1_5$ ceramics, *Int. J. Appl. Ceram. Technol.* **7**, E114 (2010).

[5]L. Yang, X. Kong, F. Li, H. Hao, Z. Cheng, H. Liu, J. F. Li and S. Zhang, Perovskite lead free dielectrics for energy storage applications, *Prog. Mater. Sci.* **102**, 72 (2019).

[6]Y. T. Cui, X. H. Fu and K. Yan, Effects of Mn-doping on the properties of $BaBi_4Ti_4O_{15}$ bismuth layer structured ceramics, *J. Inorg. Organomet. Polym.* **22**, 82 (2012).

[7]Y. J. Hao, W. Li, J. Zhai and H. Chen, Progress in high-strain perovskite piezoelectric ceramics, *Mater. Sci. Eng. R Rep.* **135**, 1 (2019).

[8]T. Takenaka and H. Nagata, Current status and prospects of lead-free piezoelectric ceramics, *J. Eur. Ceram. Soc.* **25**, 2693 (2005).

[9]X. J. Fan, Y. Wang and Y. J. Jiang, Structure and electrical properties of MnO_2-doped $Sr_{2-x}Ca_xNaNb_5O_{15}$ lead-free piezoelectric ceramic, *J. Alloy Compd.* **509**, 6652 (2011).

[10]E. Sun and W. Cao, Relaxor-based ferroelectric single crystals: Growth, domain engineering, characterization and applications, *Prog. Mater. Sci.* **65**, 124 (2014).

[11]Z. Y. Li, X. Y. Zhang, J. F. Hou and K. C. Zhou, Molten salt synthesis of anisometric $Sr_3Ti_2O_7$ particles, *J. Crystal Growth* **305**, 265 (2007).

[12]J. Wu, Y. Chang, W. Lv, G. Jiang, Y. Sun, Y. Liu, S. Zhang, B. Yang and W. Cao, Topochemical transformation of single crystalline $SrTiO_3$ microplatelets from $Bi_4Ti_3O_{12}$ precursors and their orientation-dependent surface piezoelectricity, *Crystengcomm.* **20**, 3084 (2018).

[13]L. Jin, Y. Huang, L. Zhang, J. Qiao, Z. He, R. Jing, Q. Hu, H. Du, L. Zhang, Y. Chang, X. Wei and Y. Yan, Formation mechanism of barium titanate single crystalline microplates based on topochemical transformation using bismuth-based precursors, *Ceram. Int.* **47**, 4543 (2021).

[14]Y. Ou, J. Shi, Q. Yan, C. Li and Y. Zheng, Ethanol-assisted molten salt synthesis of $Bi_4Ti_3O_{12}/Bi_2Ti_2O_7$ with enhanced visible light photocatalytic performance, *Inorg. Chem. Commun.* **133**, 108867 (2021).

[15]S. Cao, Q. Chen, Y. Li, C. Wu, J. Xu, G. Cheng and F. Gao, Novel strategy for the enhancement of anti-counterfeiting ability of photochromic ceramics: Sm^{3+} doped $KSr_2Nb_5O_{15}$ textured ceramics with anisotropic luminescence modulation behavior, *J. Eur. Ceram. Soc.* **41**, 4924 (2021).

[16]E. E. Mohammad, A. Mehdi and S. Ahmad, Synthesis of high aspect ratio platelet $SrTiO_3$, *J. Am. Ceram. Soc.* **88**, 2129 (2005).

[17]P. Xue, H. Wu, W. Xia, Z. Pei, Y. Lu and X. Zhu, Molten salt synthesis of $BaTiO_3$ nanorods: Dielectric, optical properties, and structural characterizations, *J. Am. Ceram. Soc.* **102**, 2325 (2019).

[18]F. K. Lotgering, Topotactical reactions with ferromagnetic oxides having hexagonal crystal structures, *J. Inorg. Nucl. Chem.* **9**, 113 (1959).

[19]Y. C. Liu, Y. F. Chang, E. Sun, F. Li, S. T. Zhang, B. Yang, Y. Sun, J. Wu and W. W. Cao, Significantly enhanced energy-harvesting performance and superior fatigue-resistant behavior in [001]c-textured $BaTiO_3$-based lead-free piezoceramics, *ACS Appl. Mater. Interfaces* **10**, 31488 (2018).

[20]M. R. Winter, C. B. DiAntonio, P. Yang and T. P. Chavez, Electrical properties of $Bi_4Ti_3O_{12}$ textured by screen printing, *J. Electroceram.* **26**, 1 (2011).

[21]J. L. Huang, L. Li, Y. Gu and Q. Li, Influences of progressing parameters on flake $BaBi_4Ti_4O_{15}$ powder synthesized by molten salt synthesis method, *Int. Conf. Mater. Prod. Manuf. Technol.* **335**, 704 (2011).

[22]J. Fu, Y. Hou, X. Liu, M. Zheng and M. Zhu, A construction strategy of ferroelectrics by the molten salt method and its application in the energy field, *J. Mater. Chem. C* **8**, 8704 (2020).

[23]B. J. Kennedy, Y. Kubota, B. A. Hunter, Ismunandar and K. Kato, Structural phase transitions in the layered bismuth oxide $BaBi_4Ti_4O_{15}$, *Solid State Commun.* **126**, 653 (2003).

[24]B. J. Kennedy, Q. D. Zhou, Ismunandar, Y. Kubota and K. Kato, Cation disorder and phase transitions in the four-layer ferroelectric Aurivillius phases $ABi_4Ti_4O_{15}$(A=Ca, Sr, Ba, Pb), *J. Solid State Chem.* **181**, 1377 (2008).